The Sunyaev-Zel'dovich effect in the Bullet Cluster

Haukur Sigurdarson
Onsala Space Observatory
Chalmers University of Technology

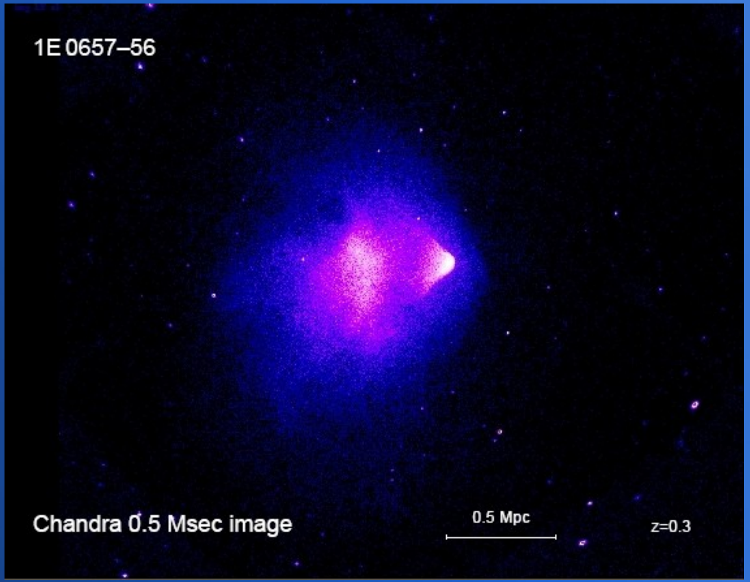

z=0.3 kT_e=13.9keV

Figure from NASA, Markevitch et al. 2005

The Sunyaev Zel'dovich effect

- Secondary anisotropy of the CMB
- Inverse Compton scattering of CMB photons by hot electrons in the cluster
- Shifts the spectrum of the CMB; the distortion has a characteristic signature
- Weak (<mK) but redshift independent (good for cosmology), depends on the amount and temperature of electrons

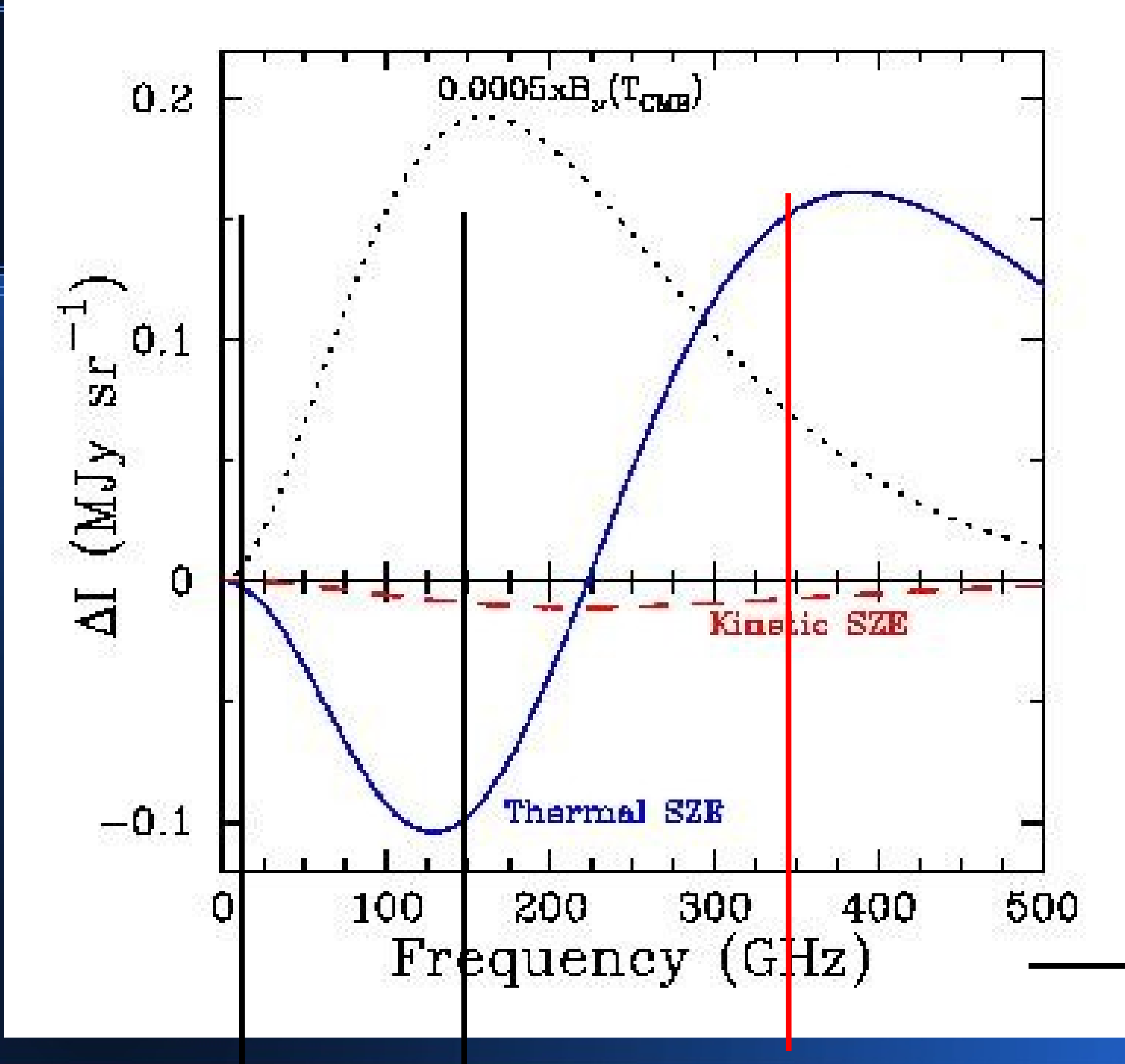

Carlstrom et al. 2002

Herschel 600-1200GHz

ATCA

APEX-SZ
SPT

APEX-Laboca

The Bullet Cluster

- A massive merger of two galaxy clusters (total mass ~10^15M_sun)
- z=0.3
- Main cluster with a “bullet” sub-cluster going through
- Dark matter, stars and gas behave differently when colliding
- The decoupling of dark matter from the gas has been observed → evidence for dark matter

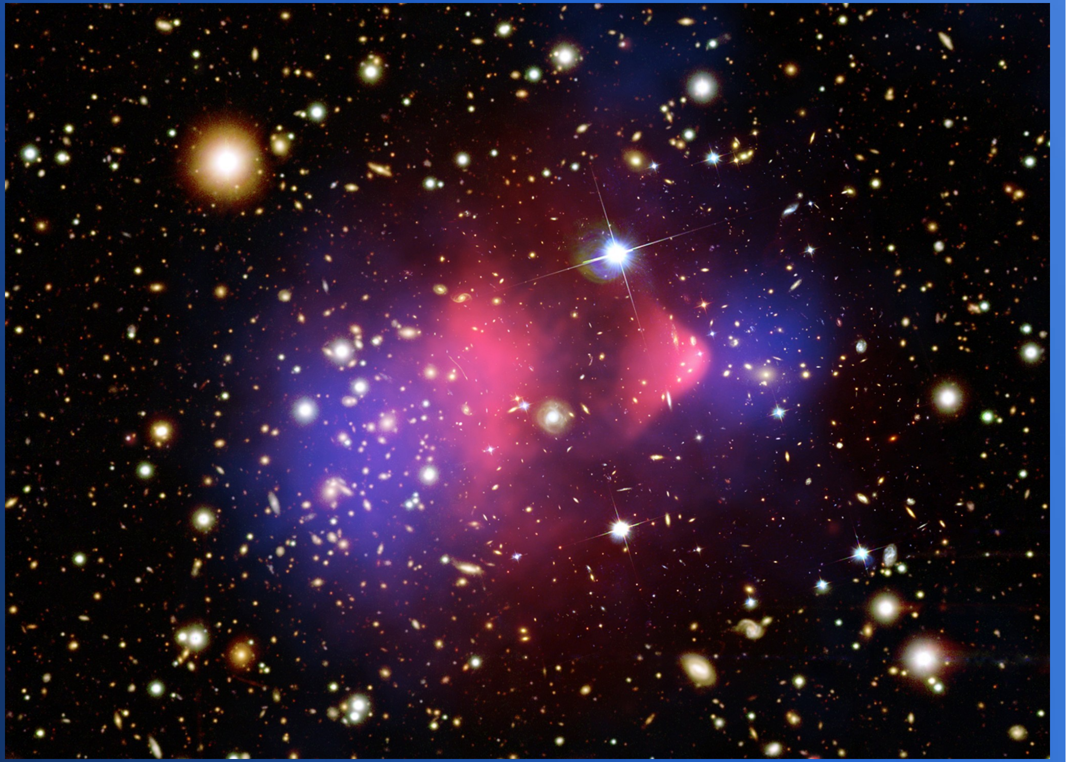

APOD 2006 August 24

Pink: X-ray
Purple: Total mass (mostly dark matter)

Previous SZ observations

Instrument	Frequency (GHz)	Angular resolution (arcseconds)	
Australia Telescope Comp. Array	18	30	Malu et al. 2010
APEX-SZ	150	60	Halverson et al. 2009
South Pole Telescope	150,220	60	Plagge et al. 2009
Herschel	600, 850, 1200	35, 25, 18	Zemcov et al. 2009
APEX-Laboca	350	>19.5	Johansson et al. 09, 10

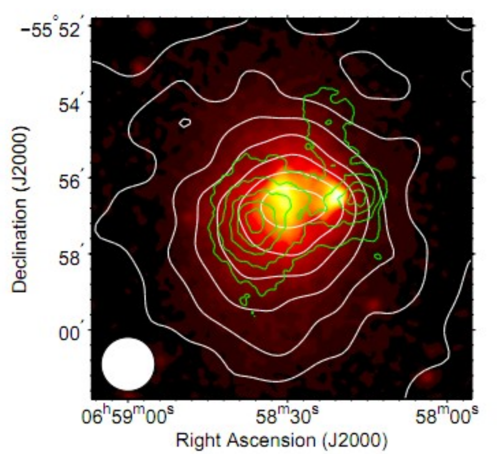

Fig. 5.— The SZE map of the Bullet system from this work, in white contours, overlaid on an X-ray map from XMM observations. The green contours show the weak lensing surface mass density reconstruction from Clowe et al. (2006). The SZE contour interval is 100 μK_{CMB}.

17 point sources (sub-mm galaxies) behind the Bullet cluster

- 3sigma~5mJy
- Highly magnified source!
- Sea of faint sources

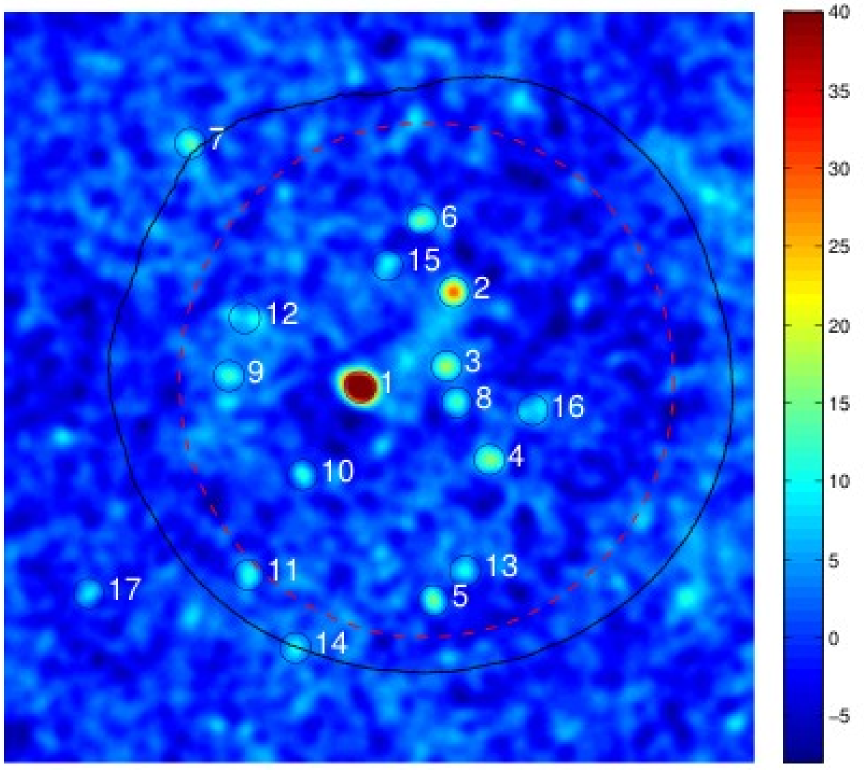

Fig. 5. Gaussian filtered map, with the 17 detected sources marked with circles. The numbering of the sources is the same as in Table 2. The black contour corresponds to the 2 mJy/beam level in the noise map and the dashed circle marks the central 10′ area of constant noise level used in the analysis.

Johansson et. al. 2010

Johansson, Sigurdarson & Horellou 2011

Detection of extended emission

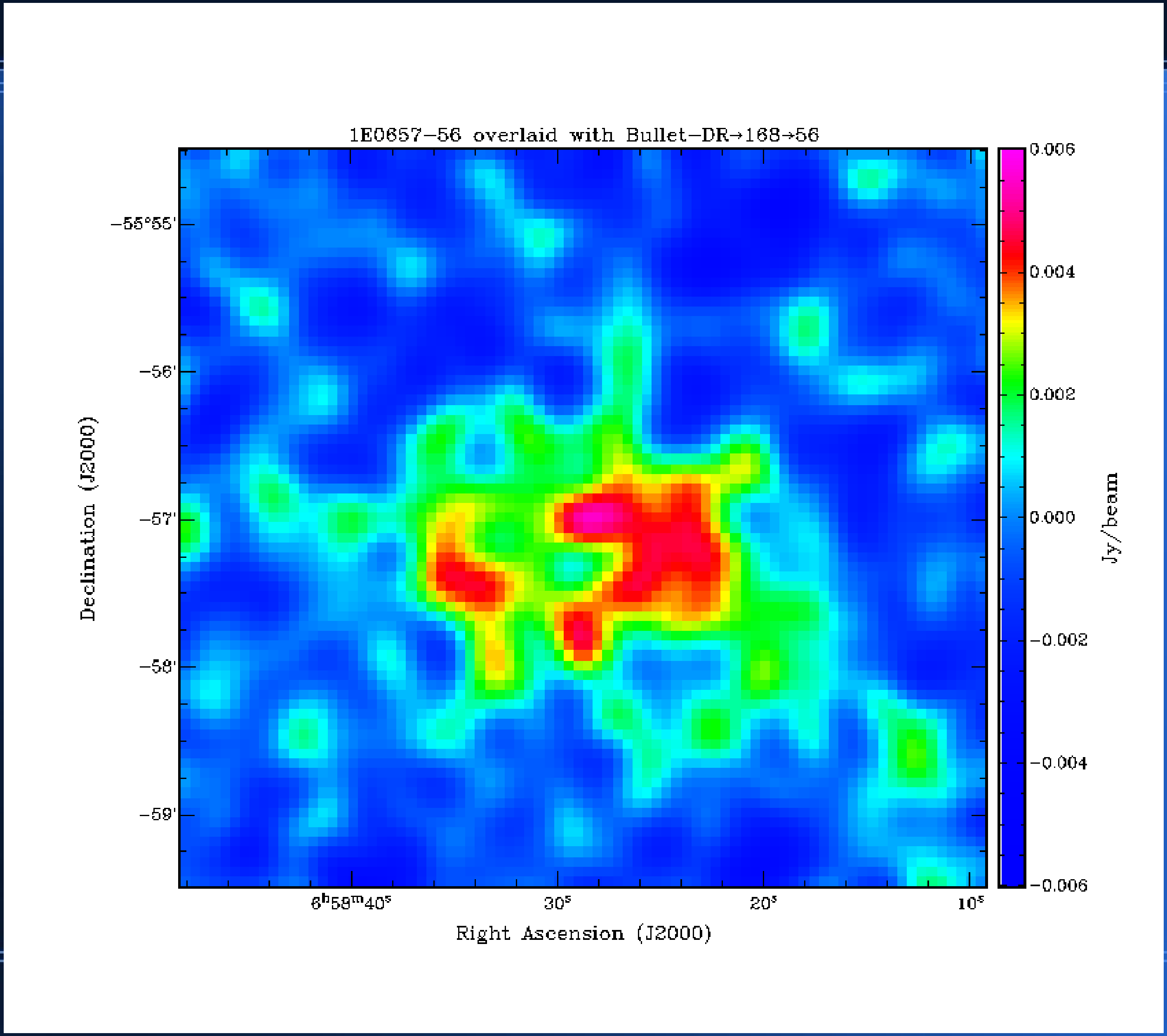

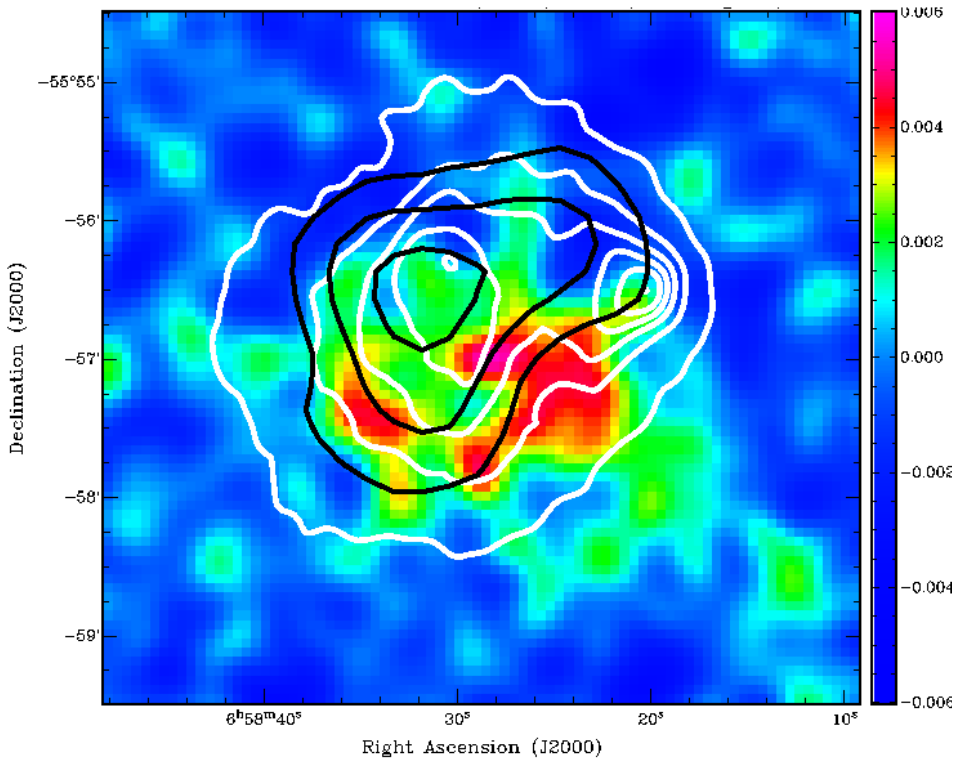

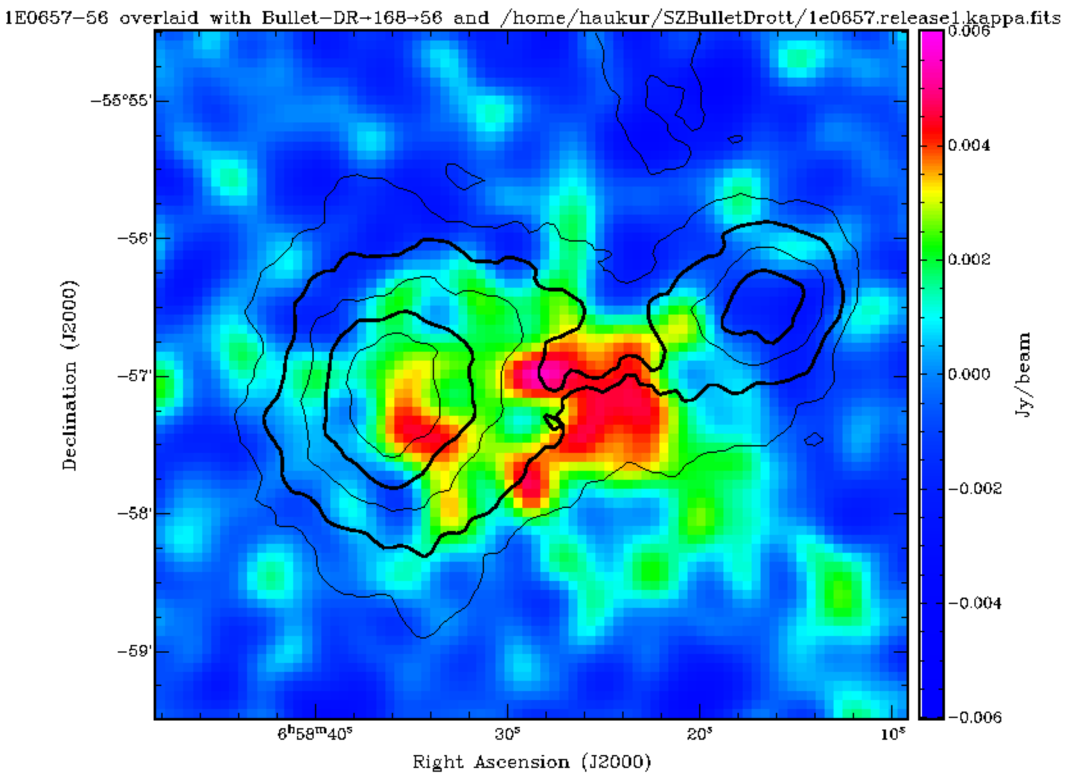

Colour: Laboca (Smoothed to 28")
Black: Halverson (85" resolution),
White: XMM

Colour: Laboca (Smoothed to 28")
Black: Total mass

SZ shifted?

- The SZ effect in the Bullet cluster seems to be shifted compared to the X-ray emission and the dark matter
- Effects of substructure?
  - X-rays sensitive to n_e^2*sqrt(T)
  - SZ traces n_e*T
- Remaining contaminating point sources?
- Effects of lensing background population of sources?

Simulation of extended SZ emission + point-like sub-mm galaxies

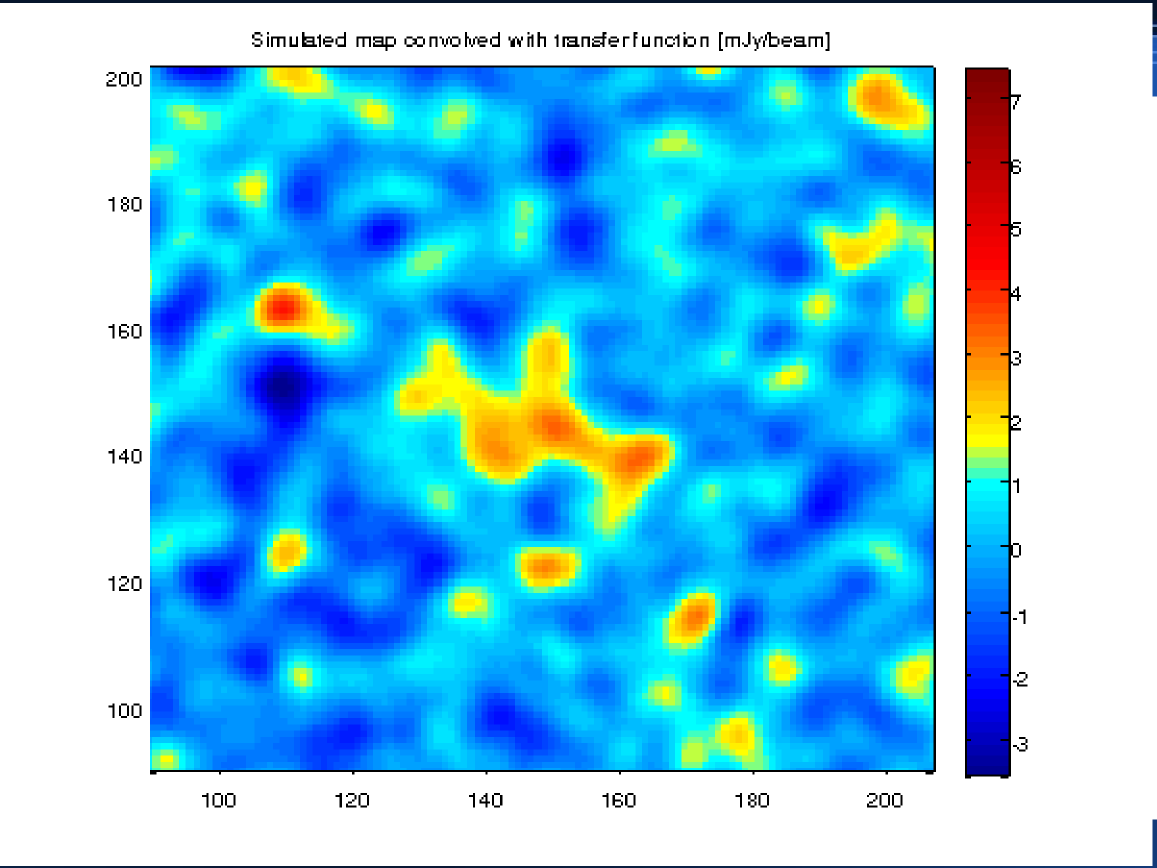

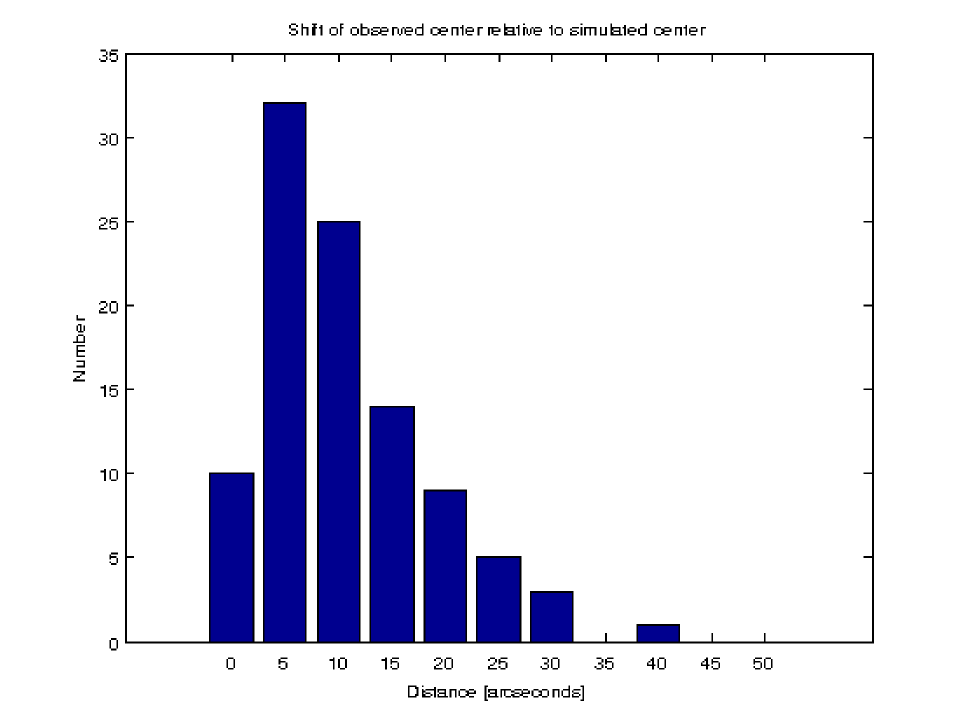

Conclusions

- High resolution observations of the SZ increment are complicated due to background sub-mm galaxies
- After removal of the brightest (>3sigma) sub-mm galaxies, we detect **extended emission** with an apparent **shift** compared to previous SZ, X-ray and weak lensing observations
- Shift due to contaminating faint sub-mm galaxies?
- Ongoing work on simulations to quantify this effect (including lensing)
- **ALMA** will be able to detect contaminating faint sub-mm galaxies

END

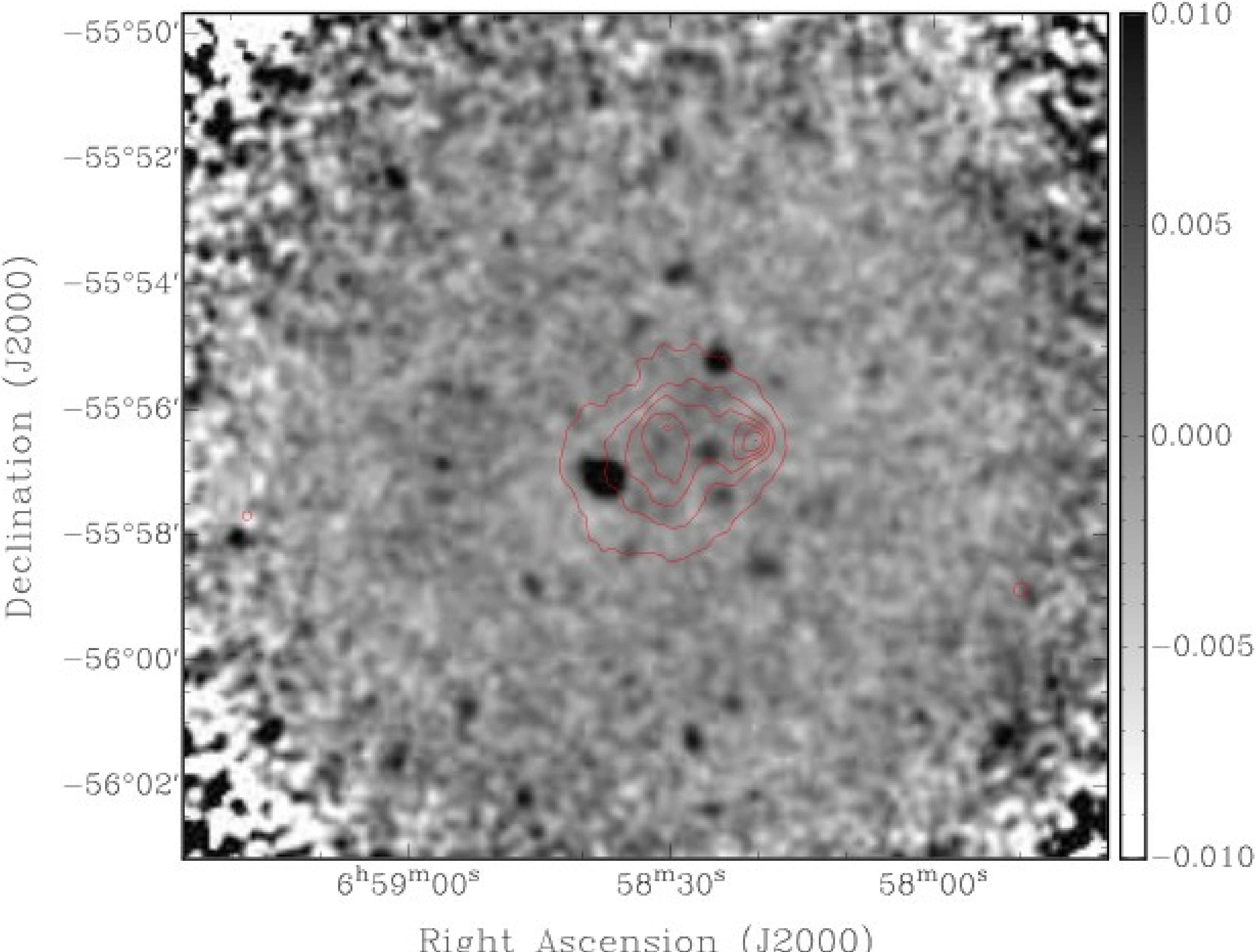

−55°50′
−55°52′
−55°54′
−55°56′
−55°58′
−56°00′
−56°02′
Declination (J2000)
6h59m00s
58m30s
58m00s
Right Ascension (J2000)
0.010
0.005
0.000
−0.005
−0.010
Jy/beam

Reduction – removing point sources

- At the Laboca frequency (345GHz) we detect high redshift (z=2-2.5) galaxies as point sources
- Many of these sources are much brighter than the SZ effect
- They must be removed so they do not contaminate
- Their positions and fluxes are found by filtering out extended emission
- Inverted versions of the sources are then inserted into the time-stream to subtract them
- This will only remove the brightest sources
- A background of faint point sources remains

APEX-SZ

- Halverson et al. 2009
- 150GHz – 1' resolution
- Fits with XMM
- Fit a beta model – used as comparison by later studies

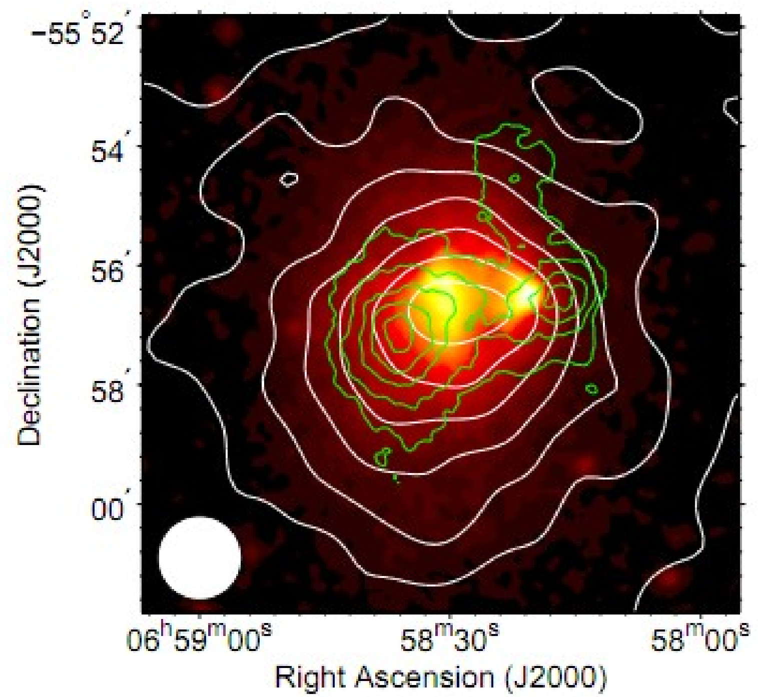

Fig. 5.— The SZE map of the Bullet system from this work, in white contours, overlaid on an X-ray map from XMM observations. The green contours show the weak lensing surface mass density reconstruction from Clowe et al. (2006). The SZE contour interval is 100 μK_{CMB}.

Herschel

- Zemcov et al. 2010
- First <650micron detection
- 18, 25, 36" resolution

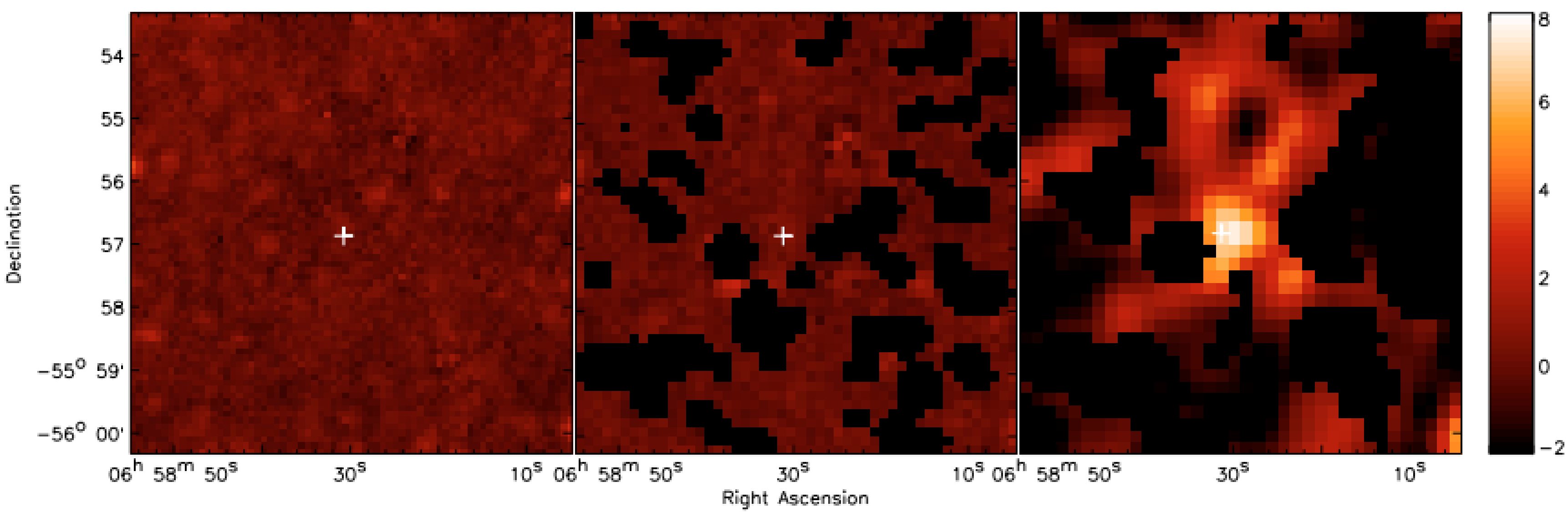

Fig. 1. Source subtracted maps at 250, 350 and 500 μm; these figures show the same regions defined by the $7' \times 7'$ green boxes in Fig. 1 of Egami et al. (2010). All three maps are shown on the colour scale shown at *right*; units are mJy beam^{-1}. The *left* most panel shows the source-subtracted 250 μm map; the confused sub-mm background is most clearly evident in this band. The *center* and rightmost panels are respectively the 350 and 500 μm source removed and masked maps; their construction is discussed in the text. The cross hairs show the best fitting SZ effect centroid from Halverson et al. (2009); the emission visible at 500 μm but not in the other maps is consistent with the position, shape and flux from the SZ effect expected at this wavelength.

Herschel

Significant at 350?

Source subtraction problem?

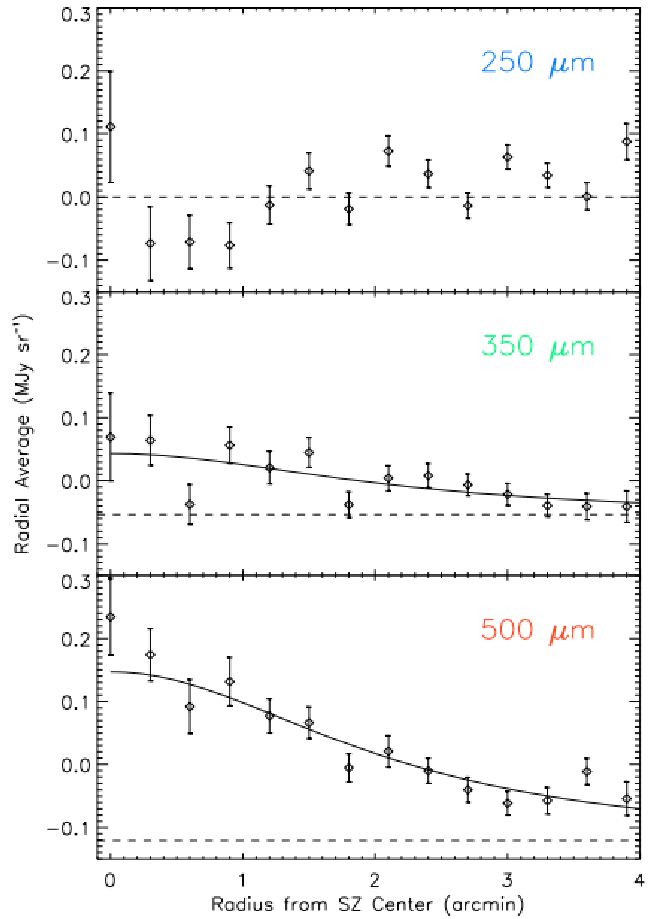

Fig. 2. Radial averages of the source subtracted and masked maps shown in Fig. 1. As the absolute mean of the maps are not measured by SPIRE, the points for each band are scattered about 0 MJy sr^{-1}. Also plotted are the best fitting isothermal β models using the parameters in Halverson et al. (2009) in the two SPIRE bands in which the SZ effect is expected to be non-zero, 350 and 500 μm; Table 1 gives the numerical values of the central increments brightnesses at both wavelengths. As the 250 μm radial bins are not correlated, each point should be compared to the (dashed) line $\Delta I = 0$ MJy sr^{-1}, while in 350 and 500 μm the dashed line shows the inferred zero level of the SZ effect.

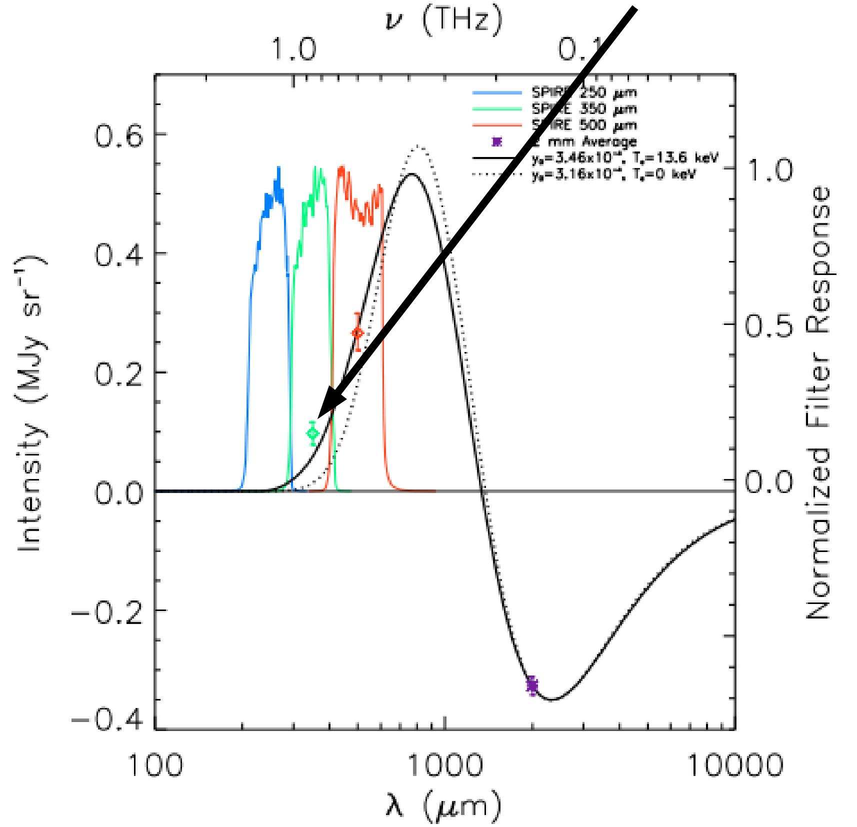

Fig. 3. The SZ effect spectrum in 1E0657−56. The 2 mm uncertainty weighted average of the measurements of Andreani et al. (1999), Halverson et al. (2009) and Plagge et al. (2010) (purple asterisk) leads to the SZ spectrum shown (solid black curve). The best fitting SPIRE measurements at 350 and 500 μm (green and red diamonds) and the normalized SPIRE bandpasses (blue, green, red solid lines) are shown for reference. The SZ effect spectrum which is consistent with the 2 mm measurements but excludes the relativistic SZ effect correction is also shown (black dotted line). Though both SZ effect curves are well matched in the decrement, the finite temperature SZ effect corrections change the results by as much as 70% of the expected signal in the SPIRE bands.

ATCA

- Malu et al. 2010
- 18GHz – 30" FWHM
- “Hole” not near X-ray peaks
- Less SZ close to X-ray peaks
- Suggest that the higher density gas is cooler – shorter cooling timescales

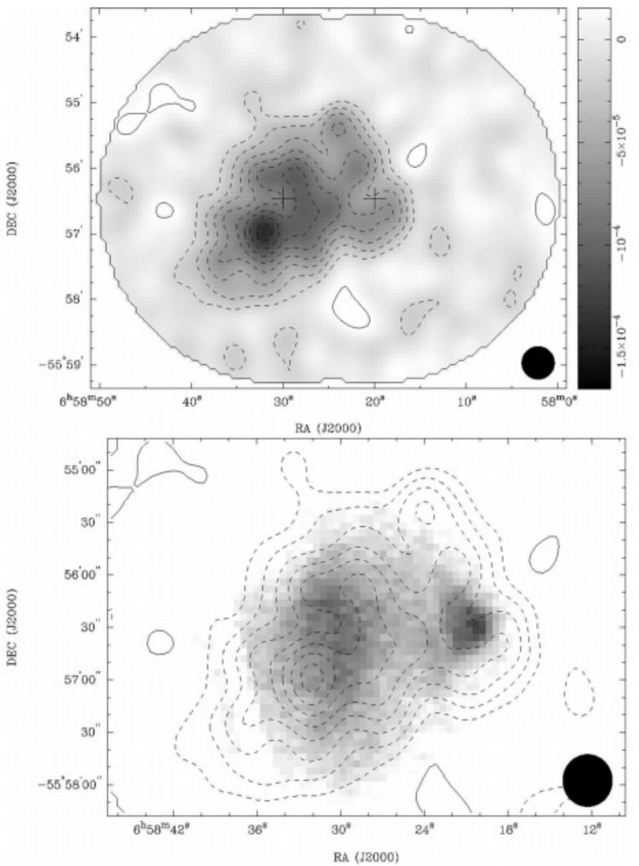

Figure 3. *Upper Panel:* Grey scales and contours represent the 18 GHz mosaic image of the SZE in the Bullet cluster; the image has been smoothed to a beam of FWHM 30$''$. Contours are at (−16, −12, −8, −6, −4, −3, −2, 2, 3) times the image rms noise of 8.4 μJy beam^{-1}. The peaks in ROSAT HRI X-ray emission are marked with cross symbols.
Bottom Panel: Contours represent the 18 GHz mosaic image of the SZE in the Bullet cluster; the image has been smoothed to a beam of FWHM 30$''$. Contours are at (−16, −12, −8, −6, −4, −3, −2, 2, 3) times the image rms noise of 8.4 μJy beam^{-1}. Grey scales represent Chandra X-ray emission.

SPT

- Plagge et al. 2010
- 150GHz, 220GHz
- ~ 1' FWHM

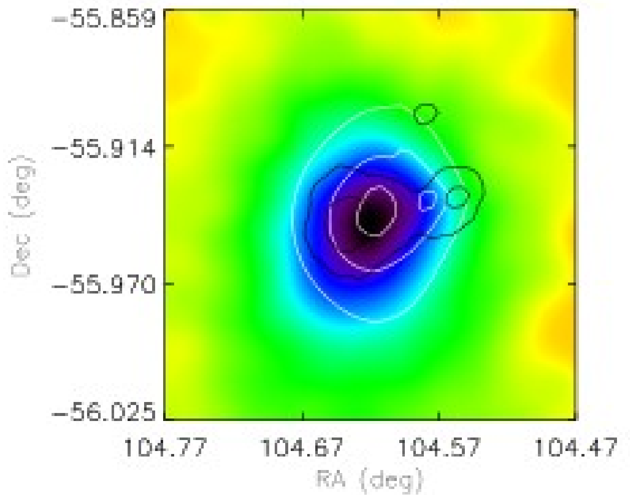

FIG. 3.— 150 GHz 1ES 0657-56 masked map with X-ray pl
density (white) and weak lensing surface mass density (black)
tours overlaid. Units are $\mu K_{\rm CMB}$. This cluster is an on
merger, and the electron gas is not in equilibrium within the
itational potential well. The SZ signal tracks the X-ray pl
density more closely than the surface mass density.

SPT

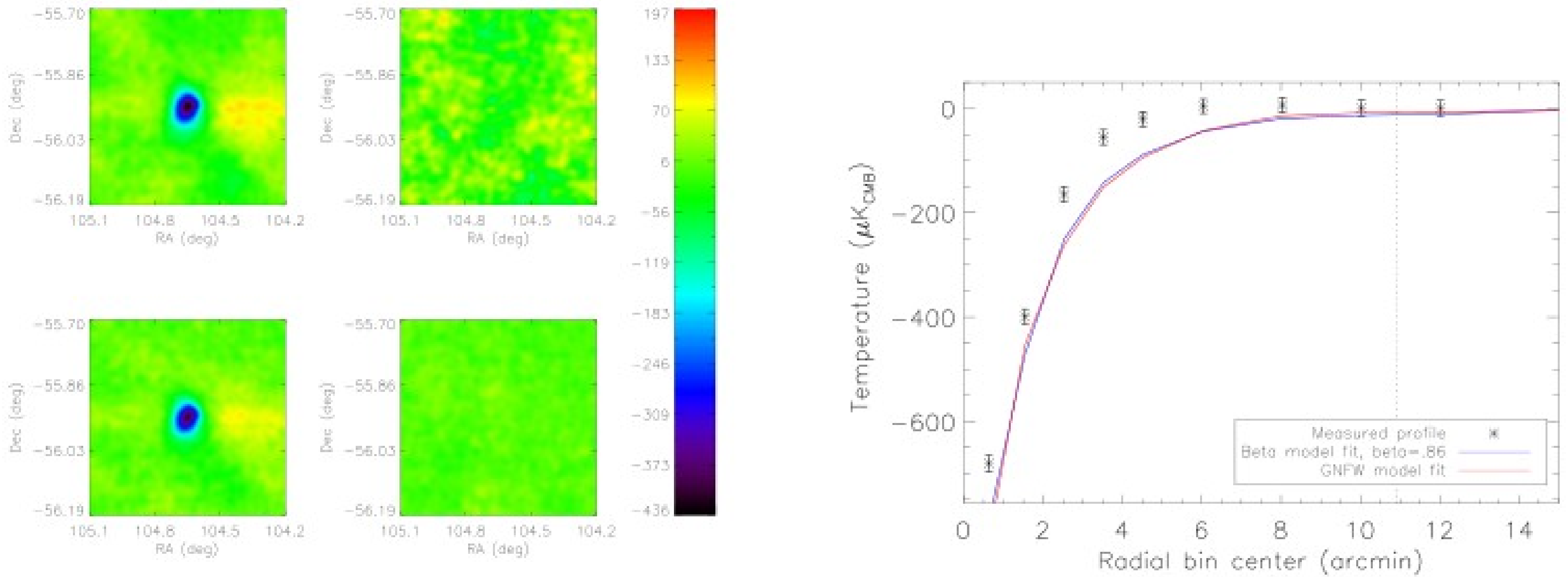

FIG. A11.— 1ES 0657-56 maps (left) and profile (right). Units are μK_{CMB}.

Transfer function

- Observation ≠ reality
- Data reduction also has a distorting effect on the data
- The effects of the telescope and data reduction can be approximated by a transfer function
- The final image is then the real data convolved with this transfer function
- Cf. dirty beam, point-spread-function